# Anionic or neutral? the charge of $Ni_8$ cubes in metal−organic framework compounds†

Ralph Freund, [ID] Andreas Kalytta-Mewes, Maryana Kraft and Dirk Volkmer [ID]*

The cubic SBU $Ni_8X_6L_6$ (X = $OH^-$/$H_2O$, L = ligand) is of great interest due to its stability and potential applications when integrated in MOFs. Here, we investigate by detailed DRIFTS measurements and exchange reactions whether it is found to be neutral in MOFs, as previously assumed in the literature, or whether it can show anionic character, as observed in complexes.

Metal−organic frameworks (MOFs) are used in a wide variety of fields, including gas storage and separation, catalysis, and biomedical and electrical applications.[1] The almost limitless pool of starting compounds and the resulting selective designability may be regarded as one of the reasons for this—depending on educts and synthesis conditions, a multitude of different MOF compounds can be generated.[2,3] The secondary building unit (SBU) plays a key role in this process, as it has a wide range of different geometries and thus not only determines the spatial orientation of the bridging ligands in the network, but also contributes significantly to the stability of the network.[4] The geometry of the SBU can accommodate a wide variety of complexities; the simplest geometries may feature only three points of extension, while more complex ones may even have 12 or more. For example, a cube-shaped SBU with $Ni(II)$ cations at the cube corners, hydroxides at the cube faces, and 12 points of extension in the form of the cube edges occupied by pyrazolates (pz) was described in terms of the anionic SBU $[Ni_8(OH)_6(pz)_{12}]^{2-}$ in various complexes (Scheme 1).[5–7] The integration of this SBU into pyrazolate-based MOFs through the use of multidentate ligands is of great interest, as they exhibit extremely high stability due to strong Ni–N coordination bonds and, due to their cubic nature, opening the door to intriguing, highly porous structures that offer numerous potential applications.[8–16] This was first achieved by Masciocchi et al.[17] where they investigated in detail

Chair of Solid State and Materials Chemistry, University of Augsburg, Institute of Physics, Universitaetsstrasse1, 86159 Augsburg, Germany.
E-mail: dirk.volkmer@physik.uni-augsburg.de

the nature of the face-bridging ligands and hence the charge of the network (neutral or anionic), as the charge is elementary for its characteristics. They concluded that the SBU is neutrally integrated into the studied MOF with $4OH^-$ and $2H_2O$ ligands on the cube faces. All subsequent publications were published under the assumption that the obtained SBUs are neutrally integrated into networks, even though this contrasts with the nature of the published pyrazolate complexes.[8–21] However, it is of fundamental importance to have knowledge about the charge state of the SBU and thus of the network since this strongly influences stability and utilization. Therefore, using the 1,4-di(4′-pyrazolyl)benzene ($H_2bdp$)-based BUT-2 as an example structure, we revisited the issue in greater detail to gain better understanding of the charge of the resulting networks and to address the question of whether the $Ni_8$ SBU in MOFs is fundamentally neutral or can exhibit anionic character, as observed in the complexes.

Single crystals of $[Ni_8X_6(bdp)_6]$ (**1a**, X = $OH^-$/$H_2O$) were synthesized similar to literature known synthesis procedures.[12] For this purpose, one equivalent of $H_2bdp$ was solvothermally reacted in an autoclave with 2 equivalents of $Ni(NO_3)_2(H_2O)_6$ in a mixture of dimethylacetamide and water for several days at 160 °C. Bulk samples of $[Ni_8X_6(bdp)_6]$ (X = $OH^-$/$H_2O$) were
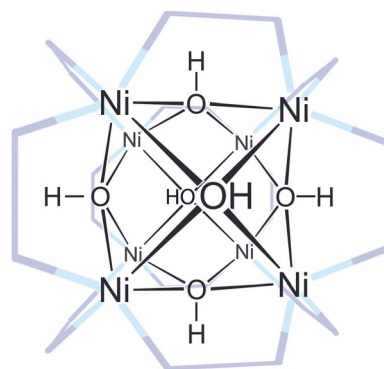


**Scheme 1** Visualisation of the anionic SBU with 6 $OH^-$ bridging the faces of the $Ni_8$ cube. The edge bridging linkers are indicated by the purple lines.
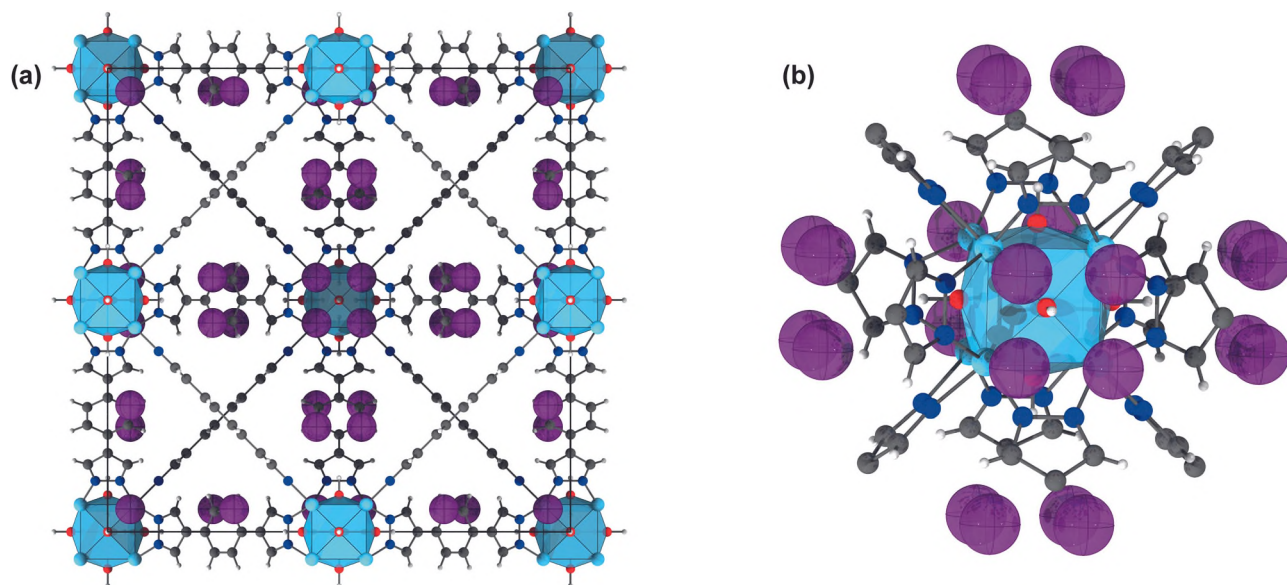
Fig. 1 (a) Visualization of the unit cell of **2a** along the a axis. (b) Visualization of the SBU of **2a** with disordered $Cs^+$ cations surrounding it with a site occupation factor of 0.073(2). Ni, light blue; O, red; C, black; H, white; N, dark blue; Cs, violet.

obtained by solvothermal reaction of 1 equivalent of $H_2bdp$ with 1.33 equivalents of $Ni(AcO)_2(H_2O)_4$ (**1b**) or $Ni(NO_3)_2(H_2O)_6$ (**1c**) in a mixture of dimethylacetamide and water in an autoclave overnight at 160 °C. Subsequent suspension of **1a, b**, and **c** in a CsOH and CsCl solution, respectively, at room temperature with repeated replacement of the metal salt solution afforded the compound $Cs_2[Ni_8(OH)_6(bdp)_6]$ (**2a, b**, and **c**).

Single-crystal X-ray diffraction of **1a, 1a** after activation at 200 °C under vacuum, and **2a** were examined at 150 K, with all the details of the structure solution and refinement being summarized in Section 8 of the ESI.† **2a** crystallizes in the cubic space group $Fm\bar{3}m$ (Fig. 1a) and a Ni : Cs ratio of 8 : 1.72 was found for the crystal examined. There are two possible explanations for the deviation from the expected Ni : Cs ratio of 8 : 2: either the network is initially neutral and is converted to the anionic form $Cs_{1.72}[Ni_8(OH)_{5.72}(H_2O)_{0.28}(bdp)_6]$ by reaction with cesium;[14] or the network is anionic from the start, with cations being disordered and thus not resolved in single crystal structure analyses, and only cation exchange takes place resulting in $Cs_{1.72}(DMA^+)_{0.28}[Ni_8(OH)_6(bdp)_6]$ ($DMA^+$ = dimethylammonium). Regardless, the disordered $Cs^+$ cations can be observed arranged around the in this case anionic SBU (Fig. 1b).

The successful incorporation of the cations into the network with the expected nickel to cesium ratio of 8 : 2 for the anionic case $[Ni_8(OH)_6(bdp)_6]^{2-}$ was further demonstrated by energy-dispersive X-ray spectroscopy (EDX) measurements using different samples of **2** (see ESI† Fig. S1–S5 and Tables S1, S2). In addition, powder X-ray diffraction (PXRD) measurements of the different products were performed, which consistently showed very good agreement with the simulated data (Fig. 2d and Figs. S6–S9 in the ESI†).

Ar adsorption measurements at 77 K (Fig. 2e) have yielded BET surface areas of approximately 2150 $m^2$ $g^{-1}$ for **1b** and 1950 $m^2$ $g^{-1}$ for **2b**. This is more than previously described in literature,[9] but agrees well with the theoretical expectations obtained by calculations with iRASPA[22] and Poreblazer.[23] The difference in BET surface area between **1b** and **2b** also agrees well with expectations based on the difference in mass (0.91 *vs.* calculated 0.87, for details see ESI,† Chapter S4).

To gain a better understanding of the SBU charge, temperature-dependent diffuse reflectance infrared Fourier transform spectroscopy (DRIFTS) measurements were performed. For this purpose, theoretical calculations were first performed on SBU cluster models to get a better understanding of the expected IR-active O–H vibrations (see ESI†, Fig. S14–S22 and Chapter S7). Hereinafter, the main focus is on 5 vibrations that were highlighted in Fig. 2a–c, which shows the results of DRIFTS measurements on bulk samples of **1b, 1c**, and **2b** (see ESI† Fig. S10 for full range spectra): vibrations 2 (3589 $cm^{-1}$) and 5 (3395 $cm^{-1}$), which can be assigned to the O–H stretching vibrations of hydroxide and water, respectively, and vibrations 1 (3664 $cm^{-1}$), 3 (3534 $cm^{-1}$), and 4 (3520 $cm^{-1}$), which can be assigned to O–H stretching vibrations of hydroxide interacting with cations surrounding the SBU (1 and 4 for dimethylammonium, 3 for cesium). For the anionic case $[Ni_8(OH)_6(bdp)_6]^{2-}$, vibration 2 would be expected, as well as, depending on the cation, either vibrations 1 and 4, or vibration 3; for the neutral case $[Ni_8(OH)_4(H_2O)_2(bdp)_6]$, vibrations 2 and 5.

Fig. 2a shows the results of the DRIFTS measurements for **2b**. Here, vibrations 2, 3, and 5 can be seen at low temperatures, with vibration 5 decreasing with increasing temperature until it disappears. As expected, the cesium containing network $Cs_2[Ni_8(OH)_6(bdp)_6]$ can be described as anionic from the beginning and only adsorbed water is gradually released. Fig. 2b shows the results of the DRIFTS measurements for **1b**. A strong vibration can be seen for vibration 2, vibration 5 is
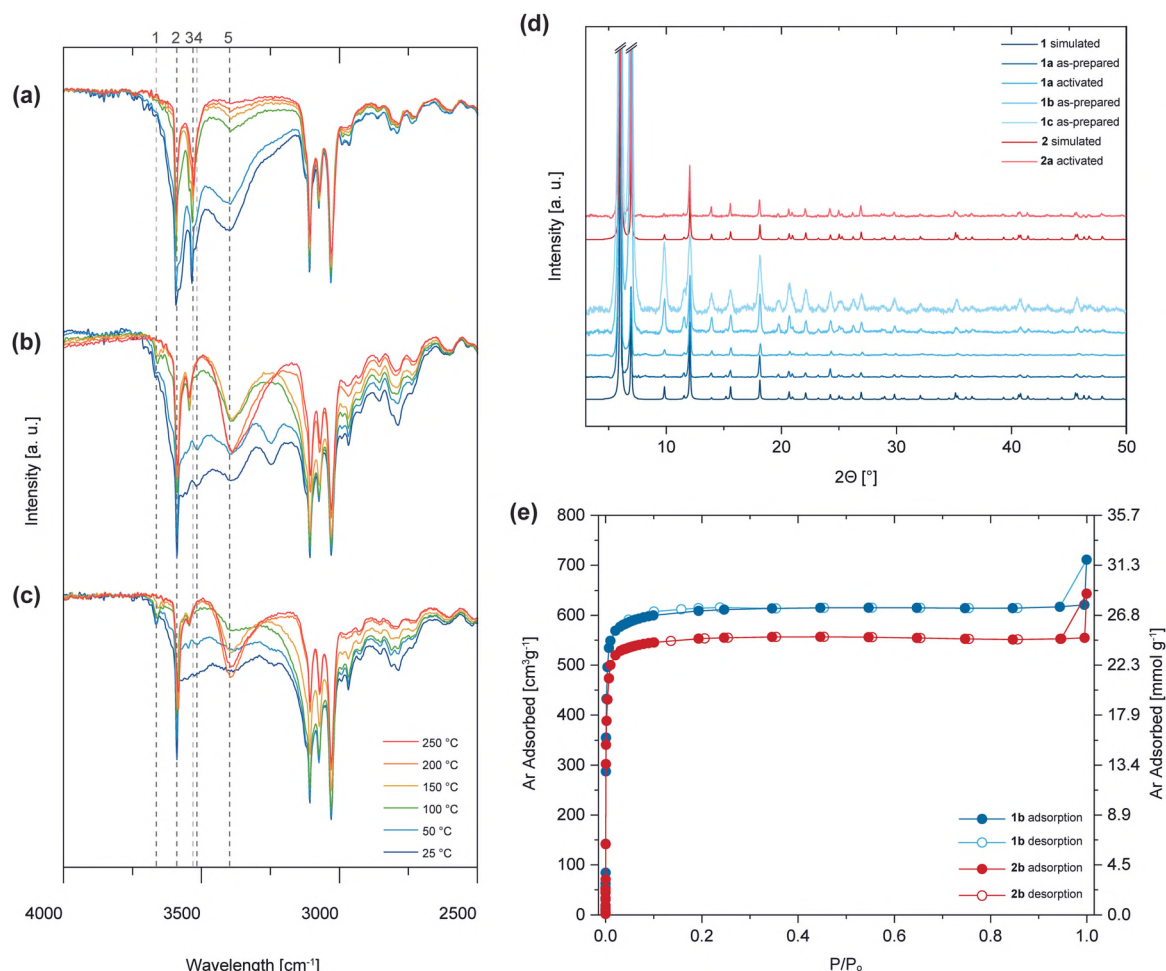
Fig. 2 Temperature dependant DRIFTS measurements for (a) $Cs_2[Ni_8(OH)_6(bdp)_6]$ (**2b**), (b) $(DMA^+)_x[Ni_8(OH)_4(H_2O)_{2-x}(bdp)_6]$ (**1b**), and (c) $(DMA^+)_2$ $[Ni_8(OH)_6(bdp)_6]$ (**1c**). (d) PXRD measurements for different single crystal and bulk samples and comparison with simulated data. (c) Ar adsorption measurements at 77 K for $[Ni_8(OH)_4(H_2O)_2(bdp)_6]$ (**1b**) and $Cs_2[Ni_8(OH)_6(bdp)_6]$ (**2b**).

weakly pronounced and becomes proportionally more intense with increasing temperature. Further, vibrations 1 and 4 can be seen weakly pronounced, disappearing at temperatures of around 100–150 °C. A similar picture emerges for **1c** in Fig. 2c, although here vibration 5 only forms at temperatures above 100 °C and vibration 1 is more pronounced. Due to the fact that in **1b**, unlike **1c**, from the beginning vibration 5 is clearly evident, we believe that **1b** is partially anionic in the form of $(DMA^+)_x[Ni_8(OH)_4(H_2O)_{2-x}(bdp)_6]$ ($x < 2$) at low temperatures, whereas **1c** is completely anionic in the form of $(DMA^+)_2[Ni_8(OH)_6(bdp)_6]$. The charge is balanced by $DMA^+$ formed during synthesis (by decomposition of dimethylaceta-mide to dimethylamine and subsequent deprotonation of the ligand) – this also explains the additional vibrations 1 and 4 which result from interaction between OH and cation (for more details see ESI† Fig. S11 and Chapters 5 and 7). At temperatures of about 150 °C and higher, an increasing decrease in 1 and 4 and increase in 5 can be observed, which can be explained by a proton transfer from dimethylammonium to the SBU, neutra-lizing it and releasing dimethylamine. This raises the question of what accounts for the different nature of SBU for **1b** and **1c**.

We believe that this can be explained by the different basicity of the anion of the metal salt: In the case of **1b**, a moderately strong base is present from the outset in the form of acetate, allowing partial deprotonation of the linker to form neutral acetic acid, whereas **1c** relies on the *in situ* formation of dimethylamine as a base, which deprotonates the linker to form cationic dimethylammonium. An analogous DRIFTS investigation as for the bulk samples was performed for the single crystal samples **1a** and **2a**, although synthesis-related impurities of $Ni(OH)_2$ could be observed here (see ESI,† Fig. S10–S12 and Chapter S5).

To verify the assumption that dimethylamine release occurs after proton transfer, and to rule out the possibility that this is a reversible system in which the proton can be transferred back to the neutralized cation after cooling, temperature-dependent mass spectrometry measurements were performed that con-firmed the expected release (see ESI,† Fig. S13 and Chapter S6 for more details).

Finally, the single crystal data of different anionic crystals were compared with an activated sample, which was expected to be neutral. Even though the protons of the water molecules

**Table 1** Overview of selected bond lengths of the single crystal measurements. **2a** 2 is a crystal taken from another batch with identical conditions as for **2a**

|  | Sum formula | Ni–Ni [Å] | Ni–O [Å] | $T$ [K] |
|---|---|---|---|---|
| **1a** | $(DMA^+)_2[Ni_8(OH)_6(bdp)_6]$ | 2.983 | 2.171 | 150(2) |
| **2a** | $Cs_{1.72}[Ni_8(OH)_6(bdp)_6]$ | 2.984 | 2.173 | 150(2) |
| **2a** 2 | $Cs_{1.34}[Ni_8(OH)_6(bdp)_6]$ | 2.980 | 2.171 | 150(2) |
| **1a** activated | $[Ni_8(OH)_4(H_2O)_2(bdp)_6]$ | 2.951 | 2.153 | 150(2) |

could not be resolved due to the statistical distribution, the comparison of the parameters showed considerable deviations. While the cell parameters for **1a** and **2a** are similar ($a$ = 25.4003(3), $\alpha$ = 90 for **1a** and $a$ = 25.3948(5), $\alpha$ = 90 for **2a**), **1a** shows a slight compression of the cell after activation at 200 °C under vacuum ($a$ = 25.3036(11), $\alpha$ = 90). This can be explained by a reduction in the dimensions of the $Ni_8$ cube due to the neutral state in comparison to the anionic SBU, as the electrostatic repulsion decreases within the SBU. An overview of selected bond lengths of the studied $[Ni_8X_6(bdp)_6]$ (X = $OH^-$/$H_2O$) structures can be found in Table 1.

With this let us return to the question posed at the beginning: anionic or neutral? The results of the network studied here have clearly demonstrated the anionic character of $[Ni_8(OH)_6(bdp)_6]^{2-}$ in the as-synthesized case. What could also be established is that the equilibrium can be shifted from the anionic to the neutral state under the right conditions. By simple means such as heating and an accompanying proton transfer, the network can be neutralized. Of course, this does not allow the conclusion that all $Ni_8$-based MOFs are anionic; similar studies must be performed for each MOF. However, at the same time, these findings open the door for further exciting investigations: The anionic state allows the incorporation of cations at defined sites into these highly porous and highly stable networks, ideal for a variety of catalytic applications.

## Conflicts of interest

There are no conflicts to declare.

## Notes and references

1 R. Freund, O. Zaremba, G. Arnauts, R. Ameloot, G. Skorupskii, M. Dincă, A. Bavykina, J. Gascon, A. Ejsmont, J. Goscianska, M. Kalmutzki, U. Lächelt, E. Ploetz, C. S. Diercks and S. Wuttke, *Angew. Chem., Int. Ed.*, 2021, **60**, 23975–24001.
2 H. Furukawa, K. E. Cordova, M. O'Keeffe and O. M. Yaghi, *Science*, 2013, **341**, 1230444.
3 M. Eddaoudi, J. Kim, N. Rosi, D. Vodak, J. Wachter, M. O'Keeffe and O. M. Yaghi, *Science*, 2002, **295**, 469–472.
4 D. J. Tranchemontagne, J. L. Mendoza-Cortés, M. O'Keeffe and O. M. Yaghi, *Chem. Soc. Rev.*, 2009, **38**, 1257–1283.
5 W. A. Al Isawi, B. M. Ahmed, C. K. Hartman, A. N. Seybold and G. Mezei, *Inorg. Chim. Acta*, 2018, **475**, 65–72.
6 Z. Wang, Z. Jagličić, L.-L. Han, G.-L. Zhuang, G.-G. Luo, S.-Y. Zeng, C.-H. Tung and D. Sun, *CrystEngComm*, 2016, **18**, 3462–3471.
7 J.-Y. Xu, X. Qiao, H.-B. Song, S.-P. Yan, D.-Z. Liao, S. Gao, Y. Journaux and J. Cano, *Chem. Commun.*, 2008, 6414–6416.
8 X.-L. Lv, K. Wang, B. Wang, J. Su, X. Zou, Y. Xie, J.-R. Li and H.-C. Zhou, *J. Am. Chem. Soc.*, 2017, **139**, 211–217.
9 N. M. Padial, E. Quartapelle Procopio, C. Montoro, E. López, J. E. Oltra, V. Colombo, A. Maspero, N. Masciocchi, S. Galli, I. Senkovska, S. Kaskel, E. Barea and J. A. R. Navarro, *Angew. Chem., Int. Ed.*, 2013, **52**, 8290–8294.
10 L. M. Rodríguez-Albelo, E. López-Maya, S. Hamad, A. R. Ruiz-Salvador, S. Calero and J. A. R. Navarro, *Nat. Commun.*, 2017, **8**, 14457.
11 K. Wang, X.-L. Lv, D. Feng, J. Li, S. Chen, J. Sun, L. Song, Y. Xie, J.-R. Li and H.-C. Zhou, *J. Am. Chem. Soc.*, 2016, **138**, 914–919.
12 Y.-Z. Zhang, T. He, X.-J. Kong, Z.-X. Bian, X.-Q. Wu and J.-R. Li, *ACS Mater. Lett.*, 2019, **1**, 20–24.
13 C. N. Neumann, S. J. Rozeveld, M. Yu, A. J. Rieth and M. Dincă, *J. Am. Chem. Soc.*, 2019, **141**, 17477–17481.
14 E. López-Maya, C. Montoro, V. Colombo, E. Barea and J. A. R. Navarro, *Adv. Funct. Mater.*, 2014, **24**, 6130–6135.
15 T. He, Y.-Z. Zhang, H. Wu, X.-J. Kong, X.-M. Liu, L.-H. Xie, Y. Dou and J.-R. Li, *Chemphyschem: Eur. J. Chem. Phys. Phys. Chem.*, 2017, **18**, 3245–3252.
16 N. Huang, K. Wang, H. Drake, P. Cai, J. Pang, J. Li, S. Che, L. Huang, Q. Wang and H.-C. Zhou, *J. Am. Chem. Soc.*, 2018, **140**, 6383–6390.
17 N. Masciocchi, S. Galli, V. Colombo, A. Maspero, G. Palmisano, B. Seyyedi, C. Lamberti and S. Bordiga, *J. Am. Chem. Soc.*, 2010, **132**, 7902–7904.
18 E. Q. Procopio, S. Rojas, N. M. Padial, S. Galli, N. Masciocchi, F. Linares, D. Miguel, J. E. Oltra, J. A. R. Navarro and E. Barea, *Chem. Commun.*, 2011, **47**, 11751–11753.
19 J. Hu, X. Deng, H. Zhang, Y. Diao, S. Cheng, S.-L. Zheng, W.-M. Liao, J. He and Z. Xu, *Inorg. Chem.*, 2021, **60**, 161–166.
20 L. Mino, V. Colombo, J. G. Vitillo, C. Lamberti, S. Bordiga, E. Gallo, P. Glatzel, A. Maspero and S. Galli, *Dalton Trans.*, 2012, **41**, 4012–4019.
21 T. He, Z. Huang, S. Yuan, X.-L. Lv, X.-J. Kong, X. Zou, H.-C. Zhou and J.-R. Li, *J. Am. Chem. Soc.*, 2020, **142**, 13491–13499.
22 D. Dubbeldam, S. Calero and T. J. Vlugt, *Mol. Simul.*, 2018, **44**, 653–676.
23 L. Sarkisov, R. Bueno-Perez, M. Sutharson and D. Fairen-Jimenez, *Chem. Mater.*, 2020, **32**, 9849–9867.